

Journal Pre-proof

Degradation of pollutants in water by Fenton-like oxidation over LaFe-catalysts:
Optimization by experimental design

Ouissal Assila, Óscar Barros, António M.F. Fonseca, Pier Parpot, Olívia S.G.P. Soares, Manuel F.R. Pereira, Farid Zerrouq, Abdelhak Kherbeche, Elizabetta Rombi, Teresa Tavares, Isabel C. Neves

PII: S1387-1811(22)00740-5

DOI: <https://doi.org/10.1016/j.micromeso.2022.112422>

Reference: MICMAT 112422

To appear in: *Microporous and Mesoporous Materials*

Received Date: 2 November 2022

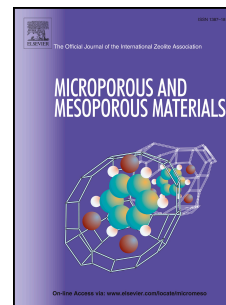
Revised Date: 20 December 2022

Accepted Date: 23 December 2022

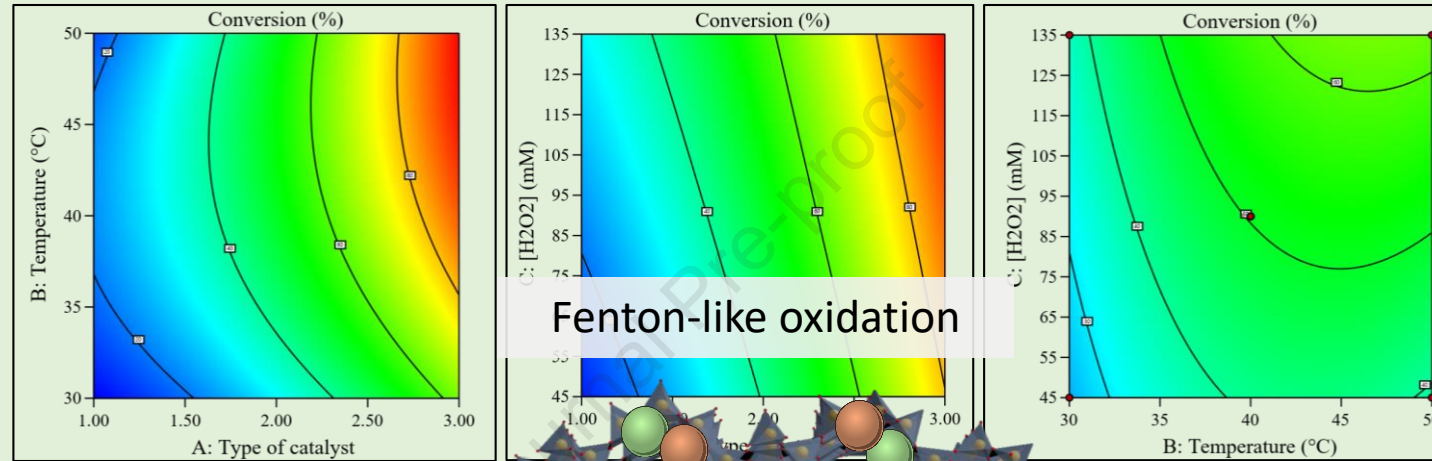
Please cite this article as: O. Assila, Ó. Barros, Antó.M.F. Fonseca, P. Parpot, Olí.S.G.P. Soares, M.F.R. Pereira, F. Zerrouq, A. Kherbeche, E. Rombi, T. Tavares, I.C. Neves, Degradation of pollutants in water by Fenton-like oxidation over LaFe-catalysts: Optimization by experimental design, *Microporous and Mesoporous Materials* (2023), doi: <https://doi.org/10.1016/j.micromeso.2022.112422>.

This is a PDF file of an article that has undergone enhancements after acceptance, such as the addition of a cover page and metadata, and formatting for readability, but it is not yet the definitive version of record. This version will undergo additional copyediting, typesetting and review before it is published in its final form, but we are providing this version to give early visibility of the article. Please note that, during the production process, errors may be discovered which could affect the content, and all legal disclaimers that apply to the journal pertain.

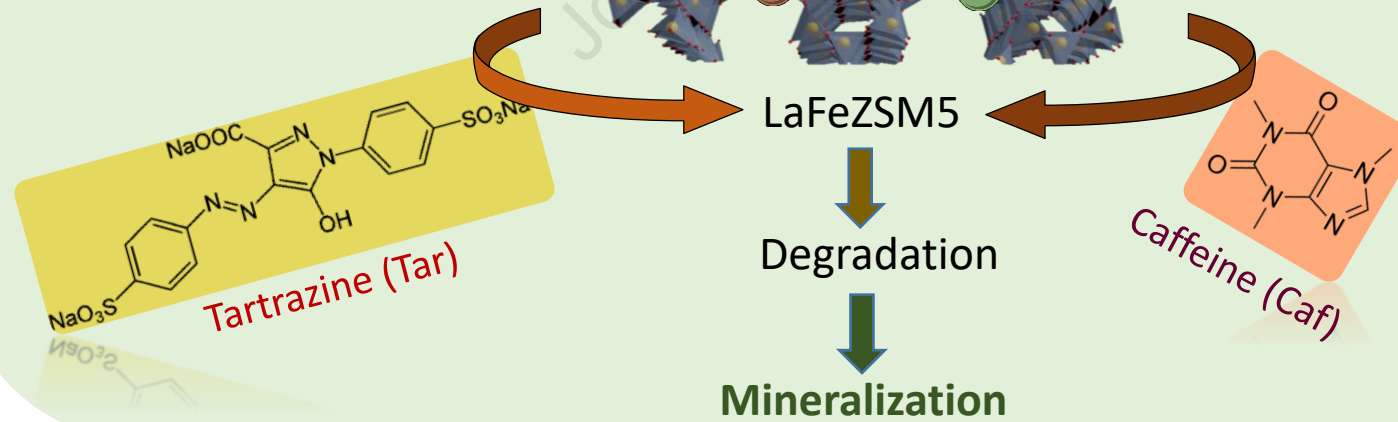
© 2022 Published by Elsevier Inc.



Box-Behnken Model: 2D response surface plots of T (°C), [H₂O₂] (mM) and type of catalyst



Fenton-like oxidation



1 **Degradation of pollutants in water by Fenton-like oxidation**
2 **over LaFe-catalysts: optimization by experimental design**

3
4 Ouissal Assila^{a,b}, Óscar Barros^{a,c,d}, António M.F. Fonseca^{a,c,d}, Pier Parpot^{a,c,d}, Olívia
5 S.G.P. Soares^{e,f}, Manuel F.R. Pereira^{e,f}, Farid Zerrouq^b, Abdelhak Kherbeche^b,
6 Elizabetta Rombi,^g Teresa Tavares^{c,d}, Isabel C. Neves^{a,c,d} *

7
8 ^a*CQUM, Centre of Chemistry, Chemistry Department, University of Minho, Campus de*
9 *Gualtar, 4710-057, Braga, Portugal*

10 ^b*Laboratory of Catalysis, Process, Materials and Environment, School of Technology,*
11 *University Sidi Mohammed Ben Abdellah Fez, Morocco*

12 ^c*CEB - Centre of Biological Engineering, University of Minho, Campus de Gualtar,*
13 *4710-057 Braga, Portugal*

14 ^d*LABELS – Associate Laboratory, Braga, Guimarães, Portugal*

15 ^e*LSRE-LCM - Laboratory of Separation and Reaction Engineering – Laboratory of*
16 *Catalysis and Materials, Faculty of Engineering, University of Porto, Portugal*

17 ^f*ALiCE - Associate Laboratory in Chemical Engineering, Faculty of Engineering,*
18 *University of Porto, Portugal*

19 ^g*Dipartimento di Scienze Chimiche e Geologiche, University of Cagliari, Complesso*
20 *Universitario di Monserrato, 09042 Monserrato, Italy*

21
22
23 *ineves@quimica.uminho.pt

24 Tel.: +351253601552 and Fax:+351253604382

1 Abstract

2 The effect of different parameters such as temperature, type of catalyst and hydrogen
3 peroxide (H_2O_2) concentration on the degradation of pollutants in water by Fenton-like
4 oxidation was studied by using the Box-Behnken design (BBD), an effective statistical
5 model to design the experiments. Concerning the heterogeneous catalysts, three
6 bimetallic catalysts with lanthanum (La) and iron (Fe) ion-exchanged into zeolites (NaY
7 and ZSM5) and a natural clay from Morocco were prepared and used for Fenton-like
8 oxidation of organic pollutants in water. Tartrazine (Tar, a food coloring compound
9 known as E102) and caffeine (Caf, a stimulant drug present in popular beverages such as
10 coffee and tea) were selected as pollutants due to their presence in several commercial
11 products for daily consumption. The BBD model indicated that the optimum catalytic
12 conditions for Fenton-like reaction with an initial pollutant concentration of 30 ppm at
13 pH 3.0 were $T = 40^\circ\text{C}$ and 90 mM of H_2O_2 . The maximum conversion values achieved
14 with the best catalyst, LaFeZSM5, were 96.6 % for Tar after 180 min and 51.0 % for Caf
15 after 300 min of reaction. To increase the conversion of Caf, a modified zeolite electrode
16 was used for electro Fenton-like oxidation without H_2O_2 , at room temperature.

17
18 **Keywords:** Box-Behnken design; $\text{La}^{3+}/\text{Fe}^{3+}$; Heterogeneous catalysts; Pollutants;
19 Fenton-like oxidation; Mineralization.

21 1. Introduction

22 Doping of inorganic materials with rare-earth ions can improve different properties,
23 making the resulting new materials very attractive for technological applications,
24 especially in the field of catalysis [1]. The rare-earth elements (REE) are a group of
25 seventeen elements (lanthanides group of the periodic table with scandium and yttrium in

1 addition). Lanthanum (La) is abundant in natural storage and could be used as a more
2 cost-effective catalyst than the other sixteen REE. Lanthanide-doped nanoparticles have
3 attracted extensive attention for their unique properties and prospective applications in
4 optical materials, photocatalysis and photonic band gap materials [1,2]. Lanthanum oxide,
5 which can contribute with both base and acid properties to the binary catalyst system, is
6 customarily used as a catalyst, co-catalyst or catalyst promoter [3–5]. La^{3+} is recognized
7 to enhance the photocatalytic activity of LaFeO_3 nanoparticles towards photodegradation
8 of dye compounds under visible light irradiation, due to the synergistic effect between the
9 semiconductor photocatalysis and the Fenton-like reaction [6]. Also, the presence of La^{3+}
10 ions in La-Na-Cu-O perovskite-like complex oxide catalysts prepared by the sol-gel auto-
11 combustion method enhances the removal of soot and simultaneously accelerates NO_x
12 reactions [7]. Recently, La-doped carbon nitride single-atom catalysts with a La-N
13 charge-transfer bridge were prepared and evaluated in the photocatalytic reduction of CO_2
14 to CO, which in turn can be converted into solar fuels. The resulting catalysts exhibited
15 high CO yielding rate, with good selectivity and stability compared to most reported
16 carbon nitride-based photocatalysts [8].

17 Several studies with REE-containing zeolites were performed in recent years to assess the
18 selectivity and stability of the catalysts [9]. The presence of REE in the Y zeolite reduces
19 the framework dealumination under hydrothermal conditions, increasing the zeolite
20 activity and enhancing the hydrogen transfer rate. One example of such is the conversion
21 of hydrocarbon fractions of crude petroleum oils to more valuable products [10,11]. In
22 addition, the ternary CuCeFeO_x catalysts supported on zeolite/PSF displayed a good
23 conversion in the oxidation of CO to CO_2 , following a pseudo-first-order kinetic law [12].
24 In the advanced oxidation processes for wastewater treatment, photocatalysis,
25 ozonization, and Fenton oxidation using metal-support as heterogeneous catalysts have

1 been applied successfully for the removal or degradation of recalcitrant pollutants [13-
2 17]. Fenton reaction is characterized by the presence of ferrous salt and hydrogen
3 peroxide to form radical hydroxyls (OH^\bullet) which turn in the rapid degradation of pollutants
4 [15-17].

5 The use of heterogeneous Fenton-like catalysts has had great attention due to their low
6 cost, eco-compatibility, operational mild conditions (20-50°C, wide pH range and
7 atmospheric pressure), and high efficiency [15-19]. These heterogeneous catalysts offer
8 a great stability of the active centres, present limited leaching of metals from the catalyst,
9 are easy recoverable from the reaction medium, and can be regenerated by a suitable
10 activation procedure [15-17]. In addition, the utilization of clays or zeolites as catalysts
11 for Fenton-like reaction is very attractive, due to the selective sorption capacities, non-
12 toxic nature, availability, and low cost [15-17,19,20] of these porous materials.

13 La-Fe montmorillonite was prepared by a precipitation method to work as a
14 heterogeneous catalyst on the degradation of rhodamine B (RhB) and methylene blue
15 (MB) dyes, using Fenton-like oxidation in both batch and fixed-bed set-ups. The catalyst
16 exhibited high dye conversions, with 96 % and 97 % degradation of the RhB and MB
17 initially present (100 mg/L), respectively [19]. In the case of zeolites, Cu(II) or Mn(II)
18 were ion-exchanged together with Fe(III) ions in NaY zeolite and used as bimetallic
19 catalysts in Fenton-like oxidation for removing two dye compounds (procion yellow (PY)
20 and tartrazine (Tar)). CuFe-NaY and MnFe-NaY displayed the best mineralization rates
21 for PY and for Tar degradation [20].

22 The goal of this work is to select the best heterogeneous catalyst based in two zeolite
23 structures, MFI and FAU, and a natural clay from Morocco, with La and Fe for the
24 degradation of tartrazine (Tar) and caffeine (Caf) pollutants in water by Fenton-like
25 oxidation. For this study, the experimental reaction conditions were optimized using a

1 statistical model. The Response Surface Methodology (RSM) is a statistical approach to
2 analyze and reduce the number of experiments to give the optima of independent
3 parameters in the reaction [21,22]. Central composite, Doehlert and Box-Behnken design
4 (BBD) are three classes of response surface designs. Box-Behnken design is more
5 advantageous than the others since it makes the experiments economically feasible and
6 beneficial for optimization of different organic matter treatment processes [23].
7 Bearing this in mind, the work was performed in four phases: (i) preparation of the
8 heterogeneous catalysts by ion-exchanging La(III) and Fe(III) into the solid supports; (ii)
9 optimization of the experimental conditions for Fenton-like oxidation using the BBD
10 model; (iii) evaluation of the stability and reusability of the best catalyst for both
11 pollutants, and (iv) performance of electro Fenton-like oxidation using the best catalyst
12 as a modified electrode to enhance the degradation of the Caf pollutant. The best catalyst
13 selected from BBD model was LaFeZSM5, which presents high degradation of Tar by a
14 typical Fenton-like oxidation. Finally, the degradation of Caf was enhanced using the
15 electro Fenton-like oxidation at room temperature without hydrogen peroxide (H₂O₂).

16

17 **2. Experimental**

18 **2.1. Materials and chemicals**

19 (NH₄)ZSM5 (CBV3024E, Si/Al = 15.00), NaY (CBV100, Si/Al = 2.83) zeolites were
20 obtained from Zeolyst International in powdered form. A natural Moroccan clay was
21 achieved from the Middle Atlas region (Clay_M, where M stands for Morocco). It was
22 dried at 100°C overnight and then crushed up to 63 μm, prior to use. The compounds:
23 tartrazine (Tar, C₁₆H₉N₄Na₃O₉S₂ ≥ 90%), caffeine (Caf, C₈H₁₀N₄O₂ ≥ 99%), sodium
24 bisulphite (Na₂SO₃), hydrochloric acid (HCl, ≥ 99.5%), sodium hydroxide (NaOH, ≥
25 99.0%) and absolute ethanol (C₂H₅OH, ≥ 99.7%) were provided by Sigma Aldrich.

1 Lanthanum (III) nitrate ($\text{La}(\text{NO}_3)_3 \cdot 6\text{H}_2\text{O}$, 99.9%, Alfa Aesar), iron (III) nitrate
2 ($\text{Fe}(\text{NO}_3)_3 \cdot 9\text{H}_2\text{O}$, Aldrich), hydrogen peroxide (H_2O_2 , 30 wt%, Merck), phosphoric acid
3 (H_3PO_4 , analytical reagent, $\geq 85\%$), and oxalic acid ($\text{C}_2\text{H}_2\text{O}_4$, $\geq 99.5\%$) were used as
4 received. Deionized water was produced with an ultrapure water system (Milli-Q, EQ
5 7000).

6 **2.2. Catalyst preparation**

7 The catalysts were prepared by an ion-exchange method using the adapted procedure
8 described elsewhere [24,25]. Aqueous solutions (250 mL) containing different lanthanum
9 amounts (0.90×10^{-2} mmol for $(\text{NH}_4)\text{ZSM5}$ and Clay_M , and 2.70×10^{-2} mmol for NaY) were
10 mixed with 4 g of the pristine support at pH 4. The suspensions were stirred during 24 h
11 at room temperature. 1.5 g of the La-containing zeolite samples, LaNaY and LaZSM5 ,
12 were added to 250 mL of iron solution (4.48×10^{-2} mmol) and then submitted to the same
13 procedure as before to obtain the bimetallic LaFeNaY and LaFeZSM5 samples. In the
14 case of the Moroccan clay as the support, due to the initial presence of iron in its structure,
15 the bimetallic LaFeClay_M sample was obtained by ion exchange only with lanthanum.
16 After each ion-exchange step, the suspensions were filtered-off, washed with deionized
17 water and dried in an oven at 60°C overnight. Finally, the solids were calcined in an oven
18 at 350°C during 4 h under a dry-air stream.

19 **2.3. Characterization**

20 The textural characterization of the catalysts was performed by N_2 adsorption isotherms,
21 determined at -196°C with a Nova 4200e (Quantachrome Instruments) equipment. The
22 samples were degassed at 150°C during 3 h. The micropore volumes (V_{micro}) and
23 mesopore surface areas (S_{meso}) were calculated by the t-method. Surface areas were
24 calculated with the BET equation.

1 The morphology of the samples was characterized using a scanning electron microscope
2 (SEM, FORMAT JEOL/EO) coupled with energy-dispersive X-ray spectroscopy (EDX).
3 In order to avoid surface charging, samples were coated with gold in vacuum prior to
4 analysis, by using a Fisons Instruments SC502 sputter coater.

5 Elemental analysis was performed by inductively coupled plasma atomic emission
6 spectroscopy (ICP-AES) for the quantification of lanthanum in the liquid phase during
7 the ion-exchange method by ICP-OES spectrometer (Optima 8000, PerkinElmer). The
8 same analysis was performed to quantify the La, Fe, Si, Al and Na in the solid samples
9 with a 5110 ICP-OES spectrometer (Agilent Technologies). Solid samples (ca. 0.05 g)
10 were thermally treated at 500°C for 12 h to remove the adsorbed water and subsequently
11 placed in a platinum crucible. Then, the melting agent was added ($\text{Li}_2\text{B}_4\text{O}_7$:sample = 15:1
12 by weight), and the alkaline fusion was carried out in a muffle furnace at 1000°C for 40
13 min. After cooling of the melt, the resultant fusion bead was transferred into a beaker and
14 heated on a plate at 80°C after addition of 100 mL of 5 % HNO_3 (all the samples were
15 found to completely dissolve within 40 min). Finally, the solution was transferred into a
16 volumetric flask (250 mL) and diluted to the desired final volume with milliQ water.

17 Fourier Transform Infrared, FTIR, spectroscopy measurements of the samples were
18 carried out using a PerkinElmer Spectrum Two spectrometer, equipped with an ATR
19 accessory. A diamond prism was used as the waveguide. All spectra were recorded with
20 a resolution of 4 cm^{-1} in the wavelength region $4000\text{-}400\text{ cm}^{-1}$ by averaging 16 scans and
21 the analyses were carried out at room temperature.

22 Temperature programmed reduction (TPR) experiments were carried out in an AMI-200
23 (Altamira Instruments) apparatus. The sample (about 100 mg) was placed in a U-shaped
24 quartz tube located inside an electrical furnace and heated at 5°C min^{-1} up to 600°C under

1 a flow of 5 % (v/v) H₂ diluted with He (total flow rate of 30 cm³ (STP) min⁻¹). The H₂
2 consumption was followed by a thermal conductivity detector (TCD).

3 **2.4. Experimental design**

4 To optimize the experimental conditions for the degradation of the organic pollutants by
5 the Fenton-like reaction, a statistical approach was applied using the Box-Behnken
6 Design (BBD) model. This design expert software allowed the set of batch experiments
7 to be developed. Three factors of three levels - (i) catalysts (X_1 : LaFeNaY, LaFeClay_M
8 and LaFeZSM5), (ii) temperature (X_2 : 30°C, 40°C and 50°C) and (iii) concentration of
9 hydrogen peroxide (X_3 : 45, 90 and 135 mM) - were used to determine the model
10 coefficients in quadratic terms (Table 1). The predicted response, Y_m , represents the
11 variables Tar (Y_1) and Caf (Y_2) calculated by equation 1:

$$12 \quad Y_m = \beta_0 + \sum_{i=1}^k \beta_i X_i + \sum_{i=1}^{k-1} \sum_{j=2}^k \beta_{ij} X_i X_j + \sum_{i=1}^k \beta_{ii} X_i^2 + \varepsilon \quad (\text{Eq. 1})$$

13 where β_0 is the intercept coefficient; β_i , β_{ii} , and β_{ij} (with $i = 1, 2, 3$; $j = 1, 2, 3$) are the
14 linear coefficients, squared coefficients and interaction coefficients, respectively.
15 X_i and X_j are the coded independent variables and ε is the random error [21,23].

16
17 **Table 1:** Independent factors and levels used for Box-Behnken design for Tar and Caf
18 degradation.

Coded factor	Factor	Coded level		
		-1	0	+1
X_1	Type of catalyst	LaFeNaY (1)	LaFeClay _M (2)	LaFeZSM5 (3)
X_2	T (°C)	30	40	50
X_3	[H ₂ O ₂] (mM)	45	90	135

19

1 2.5. Catalytic tests

2 Catalytic tests were carried out in a semi-batch reactor at atmospheric pressure under
3 stirring. Prior to experiments, the catalysts were pretreated at 100°C for 2 h in an oven.
4 The semi-batch reactor was loaded with 250 mL of a 30 ppm solution of Tar or Caf, at
5 pH = 3, using 200 mg of catalyst and 5 mL of H₂O₂ at a specific concentration and
6 temperature (Table 1). The reaction was then performed under stirring at 300 rpm, during
7 180 and 300 min for Tar and Caf, respectively, due to be the best reaction time for the
8 degradation. Sampling was carried out at fixed time intervals and the reaction was stopped
9 with the addition of an excess of NaHSO₃, which instantaneously consumes the unreacted
10 H₂O₂. Catalytic tests were performed in duplicate, and the maximum deviation observed
11 in the removal of the organic pollutants was 2%.

12 The stability of the best catalyst for Tar and Caf degradation was studied using the
13 experimental catalytic conditions determined above. Four cycles were performed and
14 after each cycle the catalyst was filtered-off, washed with ethanol and dried in an oven at
15 70 °C overnight before reutilization. FTIR and SEM analyses were carried out in order to
16 verify the stability of the support structure, while the possible leaching of metals after the
17 cycle reactions was checked by EDX analyses. The amounts of La and Fe eventually
18 leached during the reaction were also measured by ICP-OES spectrometer (Optima 8000,
19 PerkinElmer).

20 After centrifugation, the solution was analyzed in order to quantify the degradation of the
21 organic pollutants with the help of UV-vis and TOC analyses. An UV-vis
22 spectrophotometer (UV-2501PC from Shimadzu) was used at the characteristic
23 wavelengths λ_{\max} = 427 nm and 272 nm for Tar and Caf, respectively [20,26,27].

1 The total organic carbon (TOC) was determined using the NPOC method, with a
2 Shimadzu's Total Organic Carbon Analyzer TOC-L, coupled with the ASI-L autosampler
3 of the same brand.

4 **2.6. Electrochemistry**

5 The best bimetallic catalyst was used as a modified electrode for the electro-Fenton-like
6 degradation of Caf at room temperature. The modified electrode was prepared by the
7 addition of 20 mg of the bimetallic catalyst to a mixture of ultra-pure water (Millipore
8 system, 18.2 MΩ cm at 20°C) and Nafion® suspension (5 wt. % Sigma-Aldrich®). The
9 resulting catalytic ink was homogeneously deposited onto the wet proofed Toray carbon
10 paper with an area of 2 cm x 2 cm. Finally, the carbon Toray paper was glued to the
11 platinum electrode using conductive carbon cement (Quintech) and was dried at room
12 temperature for 24 h.

13 Electrochemical measurements were performed as described elsewhere [24,28,29]. The
14 electroactivity of the modified electrode was investigated by cyclic voltammetry (CV) in
15 the absence and in the presence of Caf in Na₂SO₄ (0.10 M). Electro Fenton-like oxidation
16 at a constant potential of 2.0 V vs. SCE, in the presence of Caf (100 ppm), was carried
17 out in a two-compartment cell separated with an ion exchange membrane (Nafion®-417,
18 membrane thickness 0.017 inches) that separates the anode and cathode compartments.

19 A high performance liquid chromatograph (HPLC), equipped with an isocratic pump
20 (Jasco PU-980 Intelligent HPLC Pump) and a double on-line detection including an UV-
21 vis detector (Jasco Intelligent), was used for quantifying Caf at 272 nm, i.e. at the
22 maximum of Caf absorption reported in the literature [21,30,31]. An ion exchange
23 column (Aminex HPX-87H by Biorad) and a mobile phase consisting of 1.8x10⁻³ M
24 sulfuric acid with a flow of 0.8 mL/min were used for the separation of reaction products.

1 Electrolysis products from Caf degradation were identified using a HPLC-MS system
2 (Thermo LxQ) with a C-18 (150 × 4.6 mm) column. The low molecular weight organic
3 acids were identified by HPLC analysis using the same equipment described before.

4 **3. Results and Discussion**

5 *3.1. Statistical analysis and optimal conditions for pollutants degradation*

6 In order to elucidate the importance of the different parameters and to determine the
7 optimal experimental conditions for efficient oxidation by Fenton-like reaction, the Box-
8 Behnken design (BBD) model was used.

9 The experimental design for calculating the percentage of the pollutants conversion (Y,
10 Eq.1), as the response of the design experiments with three variables - type of the catalyst,
11 temperature and concentration of hydrogen peroxide - chosen for optimization the
12 degradation of pollutants by Fenton-like reaction (Table 1) were performed with three
13 central replicates. Table 2 provides the matrix for predicting the number of experimental
14 runs to obtain responses in terms of tartrazine (Tar) and caffeine (Caf) conversions, with
15 the number of the optimized factors k equal three variables and C_0 is the central value
16 using equation 2, where a total of 15 experiments were performed [26,27]. The results
17 corresponde to the combined effect of three factors in their specified range.

$$18 \quad N = 2 \times k \times (k - 1) + C_0 \quad (\text{Eq. 2})$$

19

20

- 1 **Table 2:** Box-Behnken design for the three independent variables with the conversion
 2 (%) of the compounds.

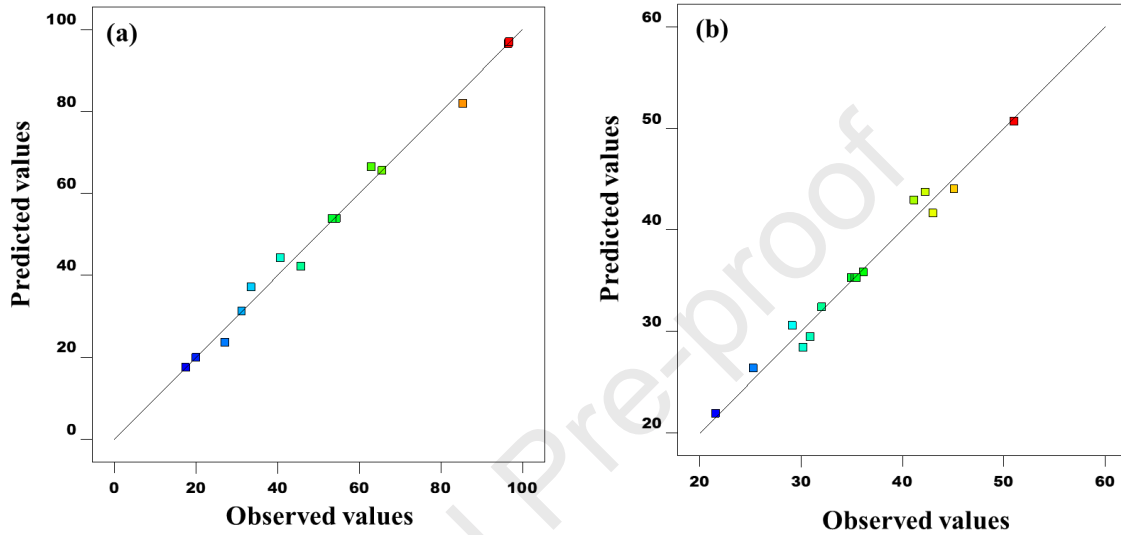
Experiments	catalyst	T (°C)	[H ₂ O ₂] (mM)	X _{Tar} (%)	X _{Caf} (%)
1	1	30	90	17.47	21.57
2	3	30	90	62.98	36.15
3	1	50	90	27.08	32.06
4	3	50	90	96.58	51.03
5	1	40	45	20.01	25.29
6	3	40	45	85.46	41.16
7	1	40	135	33.51	30.22
8	3	40	135	96.82	45.12
9	2	30	45	31.21	30.93
10	2	50	45	40.66	43.04
11	2	30	135	45.75	29.15
12	2	50	135	65.60	42.27
13	2	40	90	53.83	34.97
14	2	40	90	54.40	35.34
15	2	40	90	53.37	35.50

3

4 The analysis of variance (ANOVA) findings was carried out to evaluate the validity of
 5 the statistical model testing (Table S1). In ANOVA, the most parameters tested to assess
 6 the model validation are the ratio values of model's mean-square, the F-values signified
 7 and the confidence interval P-values of model terms were computed at 95 %, which means
 8 that P- value < 5% insured the model's significance. Hence, the higher F-values (67.67
 9 % for Tar and 27.05 % for Caf conversion), in addition to the low p-values (< 0.001) for
 10 both the pollutants, confirm that the statistical validation was of high significance.
 11 Moreover, the values of correlation coefficients (R^2) were very high (Tar: $R^2 = 0.9919$
 12 with Adj $R^2 = 0.9772$ and Caf: $R^2 = 0.9799$ and Adj $R^2 = 0.9436$, Table S1), demonstrating
 13 that the application of the developed model is well fitted to the experimental values and

1 highly predictive [34]. Furthermore, the results illustrated in Figure 1a (Tar) and 1b (Caf)
 2 revealed high correlation between the predicted and the experimental values of Tar and
 3 Caf conversions, respectively, indicating that the model is suitable and has a good
 4 performance for the response of both pollutants degradation.

5



6

7 **Figure 1.** Predicted values *versus* actual model values for (a) Tar and (b) Caf.

8 Accordingly, the second order polynomial relation that allowed also the determination of
 9 the regression between the three different factors and the response Tar (Y_1) and Caf (Y_2)
 10 conversion was expressed by equations 3 and 4:

$$11 \quad Y_1 = 53.88 + 30.47X_1 + 9.06X_2 + 8.04X_3 + 6X_1X_2 - 0.5361X_1X_3 +$$

$$12 \quad 2.6X_2X_3 + 5.15X_1^2 - 8X_2^2 - 0.0728X_3^2 \quad (\text{Eq. 3})$$

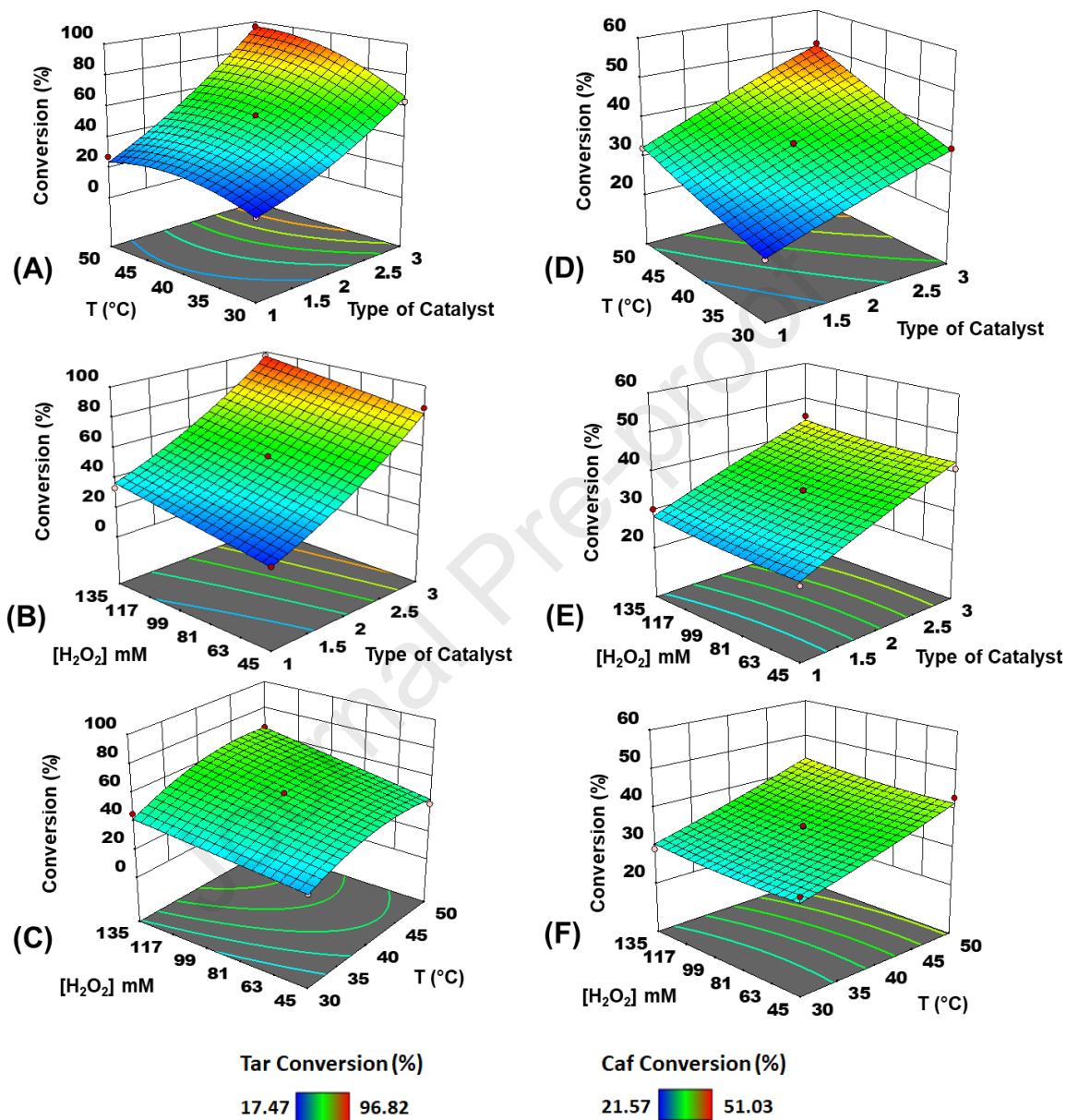
13 In the Tar degradation, the most important factor is the catalyst type, and the interaction
 14 between catalyst type and H_2O_2 concentration is not important in this case.

$$15 \quad Y_2 = 35.27 + 8.04X_1 + 6.33X_2 + 0.7925X_3 + 1.1X_1X_2 - 0.2425X_1X_3 +$$

$$16 \quad 0.2525X_2X_3 - 0.4838X_1^2 + 0.4163X_2^2 + 0.6612X_3^2 \quad (\text{Eq. 4})$$

17 For Caf degradation, it seems that the H_2O_2 concentration is not important compared to
 18 other factors.

1 Three dimensional (3D) response surface plots (RSP) for Tar and Caf degradation *versus*
 2 type of LaFe-catalyst, temperature and concentration of hydrogen peroxide are shown in
 3 Figure 2.



4
 5
 6
 7 **Figure 2.** Response Surface Plots: Effect of the three parameters studied (A, B, C for Tar
 8 conversion) and (D, E, F for Caf conversion).

9
 10 The best performances of Tar and Caf degradation by Fenton-like reaction were achieved
 11 at 40°C (Figures 2C and 2F) at pH = 3, which is considered satisfactory for a reaction

1 temperature in order to achieve the best compromise for a better degradation [20,35,36].
 2 Figures 2B (Tar) and 2E (Caf) show the effect of the initial concentration of H₂O₂ on the
 3 pollutants degradation and, when changing the concentration from 45 to 135 mM, the
 4 differences observed had similar influence on the reaction rate. Among the three catalysts
 5 used, LaFeNaY, LaFeClay_M and LaFeZSM5, RSP indicate that the conversion rate
 6 reaches the best results with the catalyst LaFeZSM5, after 180 min and 300 min for Tar
 7 and Caf, respectively (Figures 2A (Tar) and 2D (Caf)). Remarkably, the performance of
 8 the catalysts for both pollutants decreases in the order: LaFeZSM5 > LaFeClay_M >
 9 LaFeNaY.
 10 Table 3 shows the optimal conditions determined by using the Box-Behnken design for
 11 obtaining the maximum pollutants' degradation by Fenton-like oxidation.

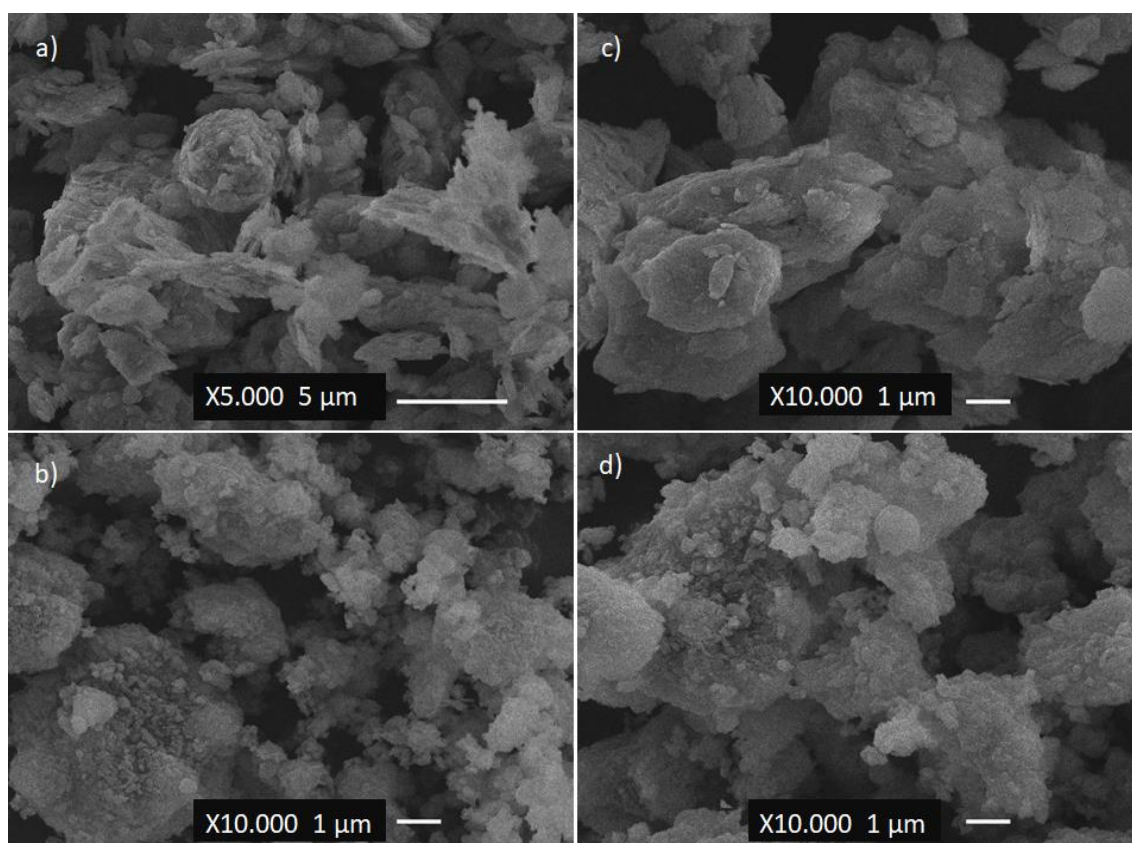
12
 13 **Table 3.** Predicted and experimental values of Tar and Caf conversion under optimal
 14 conditions.

Coded factor	Factor	Value	Optimum		Experimental	
			combination of the model (X, %)		validation of the model (X, %)	
X ₁	catalyst	LaFeZSM5	X _{Tar}	X _{Caf}	X _{Tar}	X _{Caf}
X ₂	T (°C)	40	96.56	50.66	96.60	51.00
X ₃	[H ₂ O ₂] (mM)	90				

15 X = conversion in percentage

16 The most efficient catalyst was LaFeZSM5 with a predicted degradation of up to 96.6 %
 17 of Tar and 51.0 % of Caf, after 180 min and 300 min, respectively, under the following
 18 experimental conditions: initial concentration of pollutant, 30 ppm, pH 3, H₂O₂

1 concentration, 90 mM and $T = 40^{\circ}\text{C}$. These results demonstrate that the response surface
2 methodology can be helpful as a tool to optimize the experimental conditions for the
3 degradation of pollutants mediated by Fenton-like process.
4 The introduction of the metal ions by ion-exchange method does not seem to affect the
5 morphology of the supports, as shown by scanning electron microscopy (SEM) images
6 (Figure 3).



7
8 **Figure 3.** SEM images of a) Clay_M (x5.000), b) LaFeClay_M , c) ZSM5 zeolite and d)
9 LaFeZSM5 with the same resolution (x10.000).

10

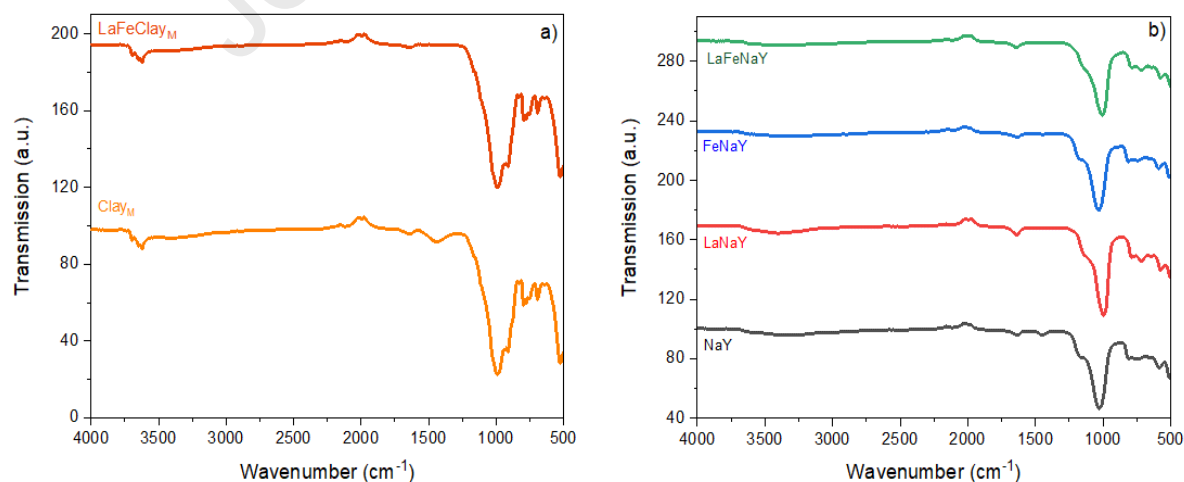
11 The heterogeneous catalysts present the same morphology of the pristine supports and
12 keep the same average particle size, indicating that the ion-exchange method is
13 appropriate. The presence of La and Fe species in the LaFe-bimetallic catalysts was also

1 investigated by energy-dispersive X-ray (EDX) analysis, which confirms the presence of
2 these metal species in the LaFe-bimetallic catalysts (Figure S1).

3 The amount of La still present in the solution after the ion-exchange process was
4 quantified by ICP-AES in order to evaluate the amount of metal loaded by the difference
5 between the initial and the final concentration. The results show that only 15 % and 30 %
6 of the initial concentration of La was ion-exchanged in ZSM5 and in Clay_M, respectively,
7 while 99 % of La was ion-exchanged in NaY. The difference in La loading between the
8 two zeolite-based samples is mainly due to the higher Si/Al ratio of ZSM5 compared to
9 NaY, which results in a lower ion exchange capacity of the former zeolite. ICP-AES
10 analyses performed on the solid catalysts to determine their chemical composition (Table
11 S2 and S3) confirm the low La content for LaFeZSM5 (0.0011 wt%) with respect to
12 LaFeNaY (0.18 wt%), whereas equal Fe contents are detected (0.26 wt% for LaFeZSM5
13 and LaFeNaY). Noteworthy, a decrease in the Si/Al ratio can be observed for the ion-
14 exchanged NaY samples, which suggests that the acidic medium affects the FAU
15 structure. In the case of the clay-supported catalyst, a low amount of La is ion-exchanged
16 (0.003 wt%), while the amount of Fe seems to be not affected by the ion exchange
17 procedure, being equal to 5.87 and 5.94 wt% for LaFeClay_M and Clay_M, respectively.

18 The intermediary catalytic behavior of LaFeClay_M determined by the BBD model could
19 be ascribed to the low amount of La and to the presence of iron most probably in the form
20 of iron oxide. It is common sense that the nature of acidic sites in clays is different from
21 those of metal oxides and zeolites [37]. In the binary acid-base CaO-La₂O₃ catalyst, the
22 different La species affect the catalytic properties, where the surface lattice oxygen in the
23 lanthanum oxide is attributed to the Lewis base sites and the metal ions La³⁺ are Lewis
24 acid sites [38]. Clay materials have higher amounts of Lewis than of Brønsted acid sites,
25 so they have a lower acidity than zeolites, despite being higher than NaY. This fact could

1 also be ascribed to the larger amount of iron present in the natural clay, 5.87 wt% for
2 LaFeClay_M, as well as to the presence of other metals, Ti (0.46 wt%) and Mg (0.71 wt%).
3 The lower activity of LaFeNaY could be assigned to the desalumination of the zeolite and
4 to the different acidic behavior of NaY zeolite. Both pristine zeolites present Brønsted
5 and Lewis acid sites characteristic of these structures with a different sites strength
6 distribution: 97 % of weak sites, 2 % medium sites and only 1 % of strong sites were
7 assessed to NaY; in the case of ZSM5, the distribution was 46.5 % of weak sites, 48.2 %
8 medium sites and 5.3 % of strong sites [39]. The higher number of strong and medium-
9 strength acidic sites of ZSM5 (53.5 %) enhances its performance compared to NaY (3 %)
10 and to the natural clay [40]. The improved efficiency of LaFeZSM5 could be attributed
11 to the fact that the presence of La species together with Fe species contributes to the acid
12 properties in the catalyst system. In addition, the presence of the iron(III) extra framework
13 increases the catalytic activity of the ZSM5 [41] as show by Fourier transform infrared
14 (FTIR) spectroscopy analysis. The typical bands of the pristine supports (Figure 4)
15 dominate all the FTIR spectra of the prepared catalysts.



16

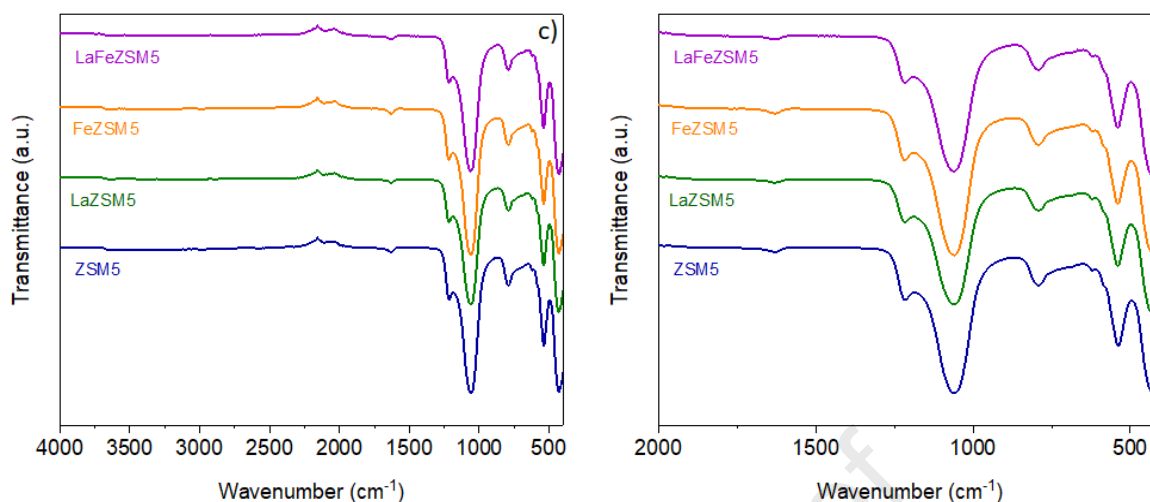


Figure 4. FTIR spectra of a) Clay_M and LaFeClay_M; b) NaY, LaNaY, FeNaY and LaFeNaY and c) ZSM5, LaZSM5, FeZSM5 and LaFeZSM5.

In the case of Clay_M, the band at 3625 cm⁻¹ is assigned to the -OH stretching vibration of the structural hydroxyl groups; the band at 1035 cm⁻¹ is due to the in-plane bending vibration of Si-O-Si and the bands at 920, 885, 850 and 520 cm⁻¹ are attributed to the stretching vibrations of (Al, Al, O)-OH, (Al, Fe, O)-OH and (Al, Mg, O)-OH, which are due to the OH groups on the edge of the clay platelets, and to the bending vibrations of Si-O-Al, respectively [42,43]. After the metal ion-exchanged, the bimetallic catalyst displays the same absorption bands at identical position (Figure 4a), which confirm that the amount of lanthanum does not affect the clay structure, in agreement of SEM analysis. For the zeolite samples, the bands in the range 3700-3000 cm⁻¹ are ascribed to surface hydroxyl groups, while the characteristic δ(H₂O) vibration mode of absorbed water corresponds to the band at 1640 cm⁻¹. Furthermore, the bands ascribable to the lattice vibrations associated with the structures are identified in the spectral region between 1300 and 450 cm⁻¹ [42,44]. The monometallic and bimetallic catalysts prepared with NaY (Figure 4b) and ZSM5 (Figure 4c) exhibit similar absorption bands as of the pristine

1 supports, suggesting that the metals ion-exchanged do not affect the zeolite structures.
2 However, the band at 1440 cm^{-1} in both NaY and Clay_M supports disappeared after metal
3 ion-exchanged in the catalysts, which could be ascribed to the presence of metal species
4 in the catalysts structure (Figures 4a and 4b).

5 Noteworthy, the absence of a band at $710\text{-}700\text{ cm}^{-1}$ in the FTIR spectrum of LaFeZSM5
6 (Figure 4c) is attributed to a migration of the Fe ions from the framework to extra-
7 framework positions [41]. The presence of La and Fe species ion-exchanged on ZSM5,
8 together with the acidity behavior of the zeolite endorse the Fenton-like oxidation for
9 degradation of Tar and Caf pollutants.

10 From TPR analysis (data not shown), a profile similar to that of the pristine support was
11 detected for the bimetallic LaFeClay_M catalyst, with a broad reduction peak centered at
12 $630\text{ }^{\circ}\text{C}$, indicating that the presence of La^{3+} does not affect the clay framework. However,
13 the bimetallic catalysts prepared with zeolites do not display any reduction peaks, due to
14 the lower amount of the metal species ion-exchanged and their good dispersion into the
15 zeolite structures. A similar behavior was observed for heterogeneous catalysts prepared
16 with palladium ion-exchanged in NaY zeolite [45].

17 N_2 adsorption/desorption isotherms acquired at -196°C for the heterogeneous catalysts
18 are described in Figure S2, where those of the pristine supports are also reported for
19 comparison. According to the IUPAC classification, both Clay_M and the bimetallic
20 catalyst present a Type IIb isotherm with a hysteresis loop, characteristic of clays with
21 mesoporous nature [46]. Type I isotherms typical for microporous solids are shown by
22 all the zeolite-based catalysts; however, the presence of some mesoporosity, especially in
23 the case of ZSM5 and the derived catalysts, is highlighted by the appearance of hysteresis
24 loops [47]. The resulting textural parameters are summarized in Table 4. It can be

1 observed from the figures that, whatever the support, the addition of La and/or Fe does
2 not modify the shape of the original isotherms.

3 **Table 4.** Physicochemical properties of the parent supports and the samples.

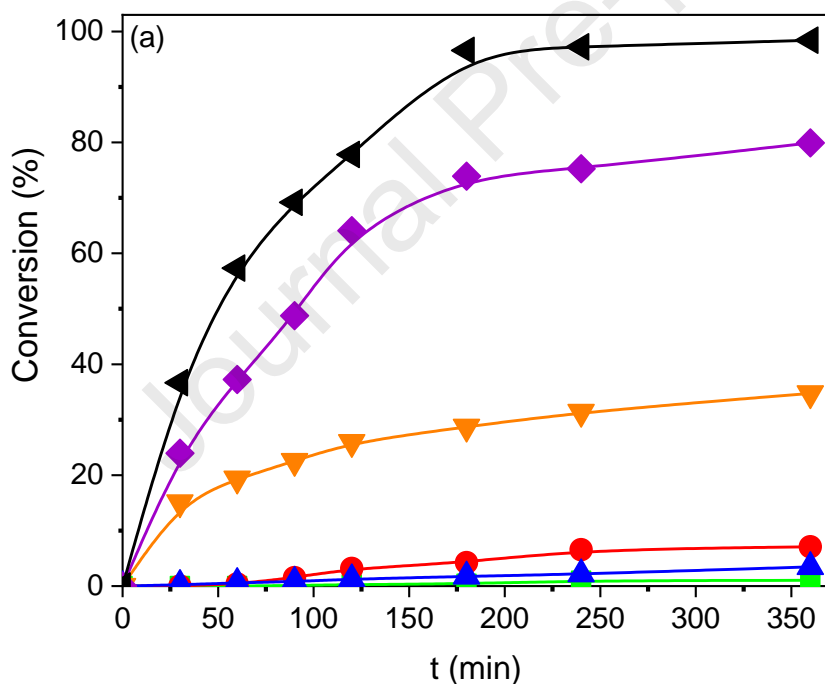
Samples	S_{BET} (m^2/g) ^a	V_{total} (cm^3/g) ^b	S_{meso} (m^2/g) ^c	V_{micro} (cm^3/g) ^c	V_{meso} (cm^3/g) ^e
Clay _M	23	0.039	23	0	0.039
LaFeClay _M	22	0.043	22	0	0.043
NaY	792	0.378	19	0.340	0.038
FeNaY	623	0.344	87	0.222	0.122
LaNaY	536	0.256	88	0.106	0.150
LaFeNaY	586	0.272	83	0.208	0.064
ZSM5	401	0.260	185	0.091	0.169
FeZSM5	347	0.197	141	0.087	0.110
LaZSM5	355	0.203	174	0.076	0.127
LaFeZSM5	347	0.201	127	0.091	0.110

4 ^aSurface area calculated from the BET equation; ^bTotal pore volume determined from the
5 amount adsorbed at $P/P_o = 0.95$; ^cExternal surface area and micropore volume calculated by the
6 t -method; ^dMesopore volume calculated by the difference $V_{\text{total}} - V_{\text{micro}}$. [48].

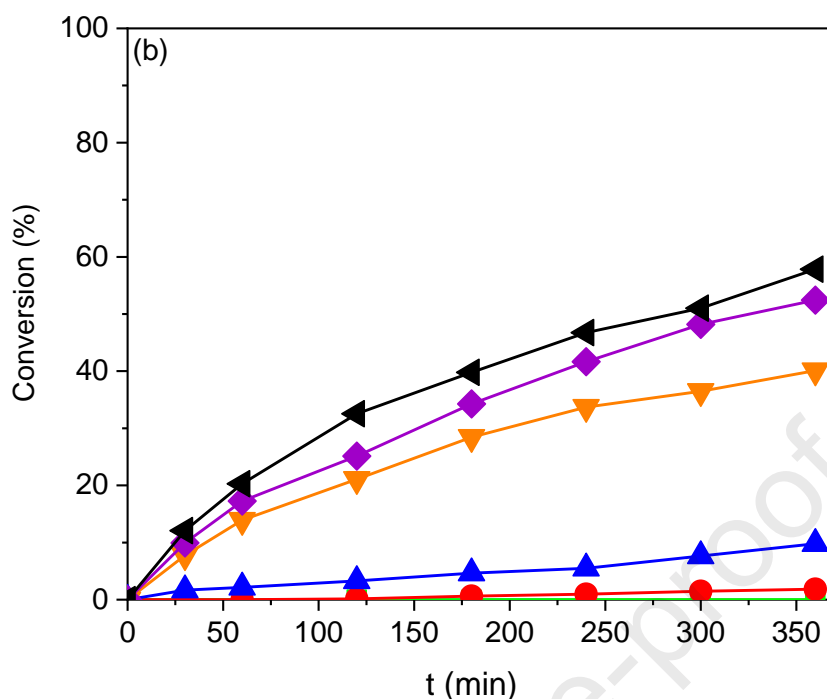
7 As expected, both the BET surface area (S_{BET}) and pore volume (V_{total}) of clays are much
8 lower compared to those of zeolites, whose values are almost unaffected after the addition
9 of La. On the other hand, a decrease in such parameters can be observed for the ion-
10 exchanged catalysts in comparison with the pristine support, for both the NaY- and
11 ZSM5-based samples. Noteworthy, in contrast with the ZSM5-based ones, the addition
12 of La and/or Fe leads to an increase in V_{meso} , for the NaY-supported samples, particularly
13 evident for the monometallic ones.

3.2. Pollutants degradation by Fenton-like oxidation with LaFeZSM5

The validation of the optimized experimental conditions was performed in order to verify the values predicted by the mathematical model. For that, ZSM5, LaZSM5, FeZSM5 and LaFeZSM5 were used as heterogeneous catalysts to check their performance in the degradation of the pollutants under the optimized experimental parameters. The influence of H_2O_2 as the oxidant in the presence of pollutants was also evaluated. Figure 5 shows the catalytic results for the Fenton-like oxidation for Tar (Figure 5a) and Caf (Figure 5b), using 0.8 g/L of catalysts, which are in significant agreement with the theoretical values indicated by the model.



10



1

2 **Figure 5.** Conversion of a) Tar and b) Caf *versus* reaction time over H₂O₂ (red curves),
 3 ZSM5 (blue curves), LaFeZSM5 (green curves), LaZSM5 + H₂O₂ (orange curves),
 4 FeZSM5 + H₂O₂ (violet curves) and LaFeZSM5 + H₂O₂ (black curves).

5

6 Control tests carried out in the presence of only hydrogen peroxide (H₂O₂ – red curves),
 7 the pristine zeolite (ZSM5 – blue curves) or the LaFeZSM5 catalyst (green curves)
 8 showed negligible conversions of both Tar and Caf.

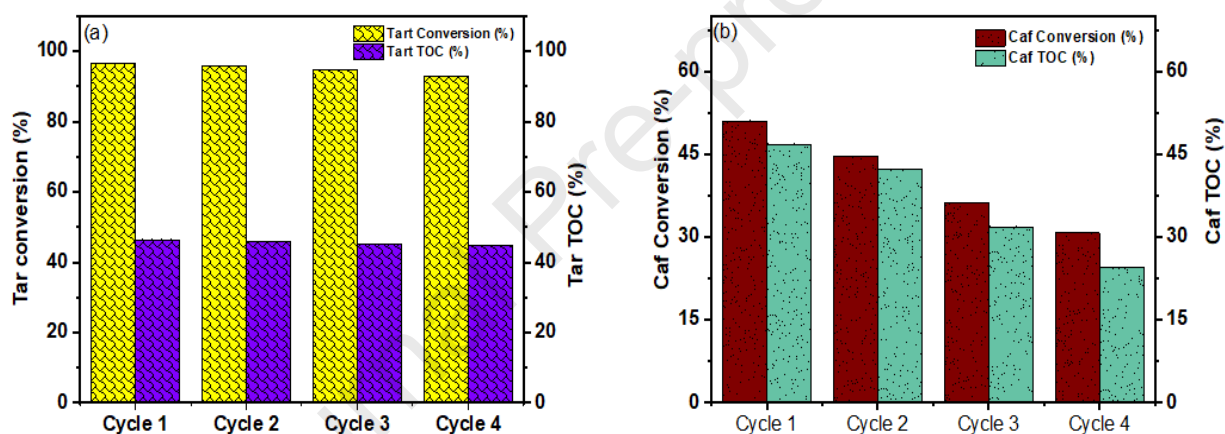
9 When H₂O₂ and the heterogeneous catalysts are simultaneously present, remarkably
 10 improved performances are obtained, proving that the reaction follows a typical Fenton-
 11 like process. For both Tar and Caf compounds the degradation by Fenton-like oxidation
 12 in the presence of the heterogeneous catalysts follows the same trend (LaZSM5 <
 13 FeZSM5 < LaFeZSM5). Concerning the monometallic catalysts, higher conversions are
 14 shown for FeZSM5 (violet curves) in comparison with LaZSM5 (orange curves), with
 15 much more notable differences in the case of Tar. This is not surprising since iron is a

1 crucial metal for Fenton reactions, as already reported in other works [15-
2 17,20,35,36,49,50]. Interestingly, for both pollutants, the catalyst LaZSM5 (orange
3 curves) shows comparable conversions with 34.7 % and 40.1 % for Tar and Caf,
4 respectively. By converse, remarkable differences in the degradation of the two pollutants
5 are observed in the presence of the bimetallic catalyst. Indeed, 96.6 % of Tar was
6 degraded after 180 min of reaction, with a mineralization efficiency of 45.5 %, whereas
7 only 58 % of Caf was converted after 300 min, with a comparable degree of
8 mineralization, 47.0 %. The highest conversion values are obtained with the LaFeZSM5
9 catalyst, indicating that the synergistic effect of the two metal ions together with the acid
10 properties of ZSM5 allow the optimal combination for achieving the best catalytic
11 performance, especially in the case of Tar.

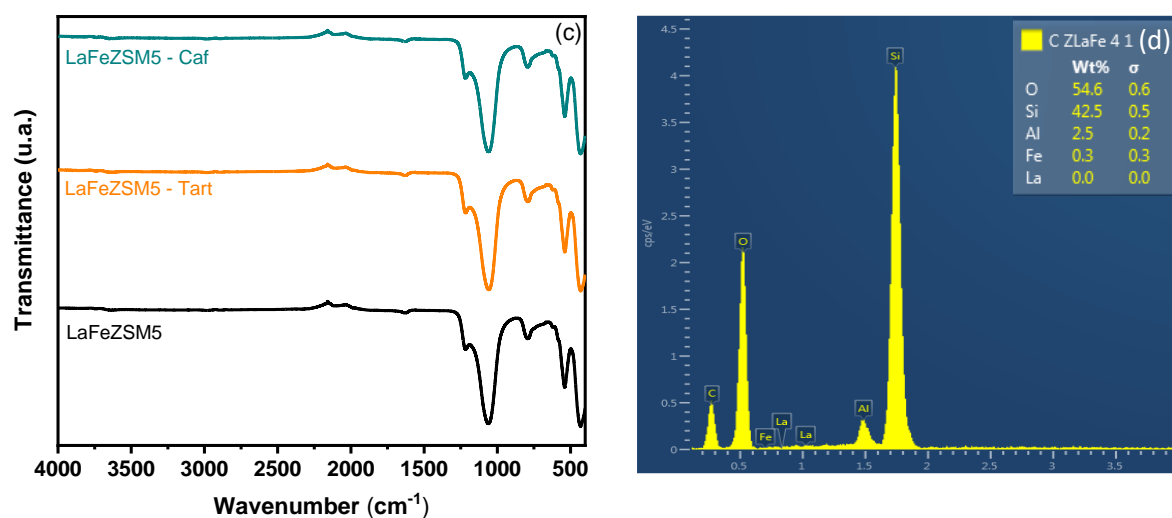
12 The stability and reusability of the best catalyst in the Fenton-like degradation of Tar and
13 Caf were studied during four cycles and at the end of each cycle TOC was quantified
14 (Figure 6). Figure 6a depicts that the bimetallic catalyst is very stable in the case of Tar,
15 with conversions above 96 % and important mineralization efficiencies of 45.5 %
16 preserved during the four cycles. On the other hand, LaFeZSM5 loses its activity in the
17 degradation of Caf, whose conversion decreases significantly after each reaction cycle
18 (Figure 6b). However, the X_{caf}/TOC ratio remains almost constant during the reusability
19 test, varying between 1.10 (1° cycle) and 1.25 (4° cycle), indicating that the catalyst
20 maintains its mineralization capacity despite the worsening of the degradation
21 performance.

22 FTIR and SEM/EDX analyses of the catalyst were performed after the fourth cycle of the
23 reusability tests in the degradation of both Tar and Caf. FTIR spectra of LaFeZSM5
24 before and after the last recycling tests are very similar to that of the pristine zeolite,

1 demonstrating the stability of the catalyst during the Fenton-like degradation (Figure 6c)
 2 and indicating that the structure of the catalyst is preserved during such reaction.
 3 After Tar degradation, EDX analysis confirms the absence of leaching phenomena for
 4 both La and Fe metal ions. In the EDX spectrum of LaFeZSM5 after Caf degradation
 5 (Figure 6d), only iron is detected, probably La is leaching. The loss of the La ions could
 6 explain the decrease in the Caf oxidation activity of LaFeZSM5, while it does not seem
 7 to affect the mineralization efficiency, as suggested by the constant value of the X_{caf}/TOC
 8 ratio.



9



10

1 **Figure 6.** Conversion and TOC percentages during the consecutive degradation cycles
2 for Tar (a) and Caf (b) over LaFeZSM5; FTIR (c) and (d) EDX spectra at the end of the
3 last cycle of Caf.

4

5 At the end of the Tar degradation, no leaching of La or Fe was detected (within the
6 experimental error), revealing that the LaFeZSM5 are stable. However, after Caf
7 degradation only Fe was detected in agreement with EDX analysis.

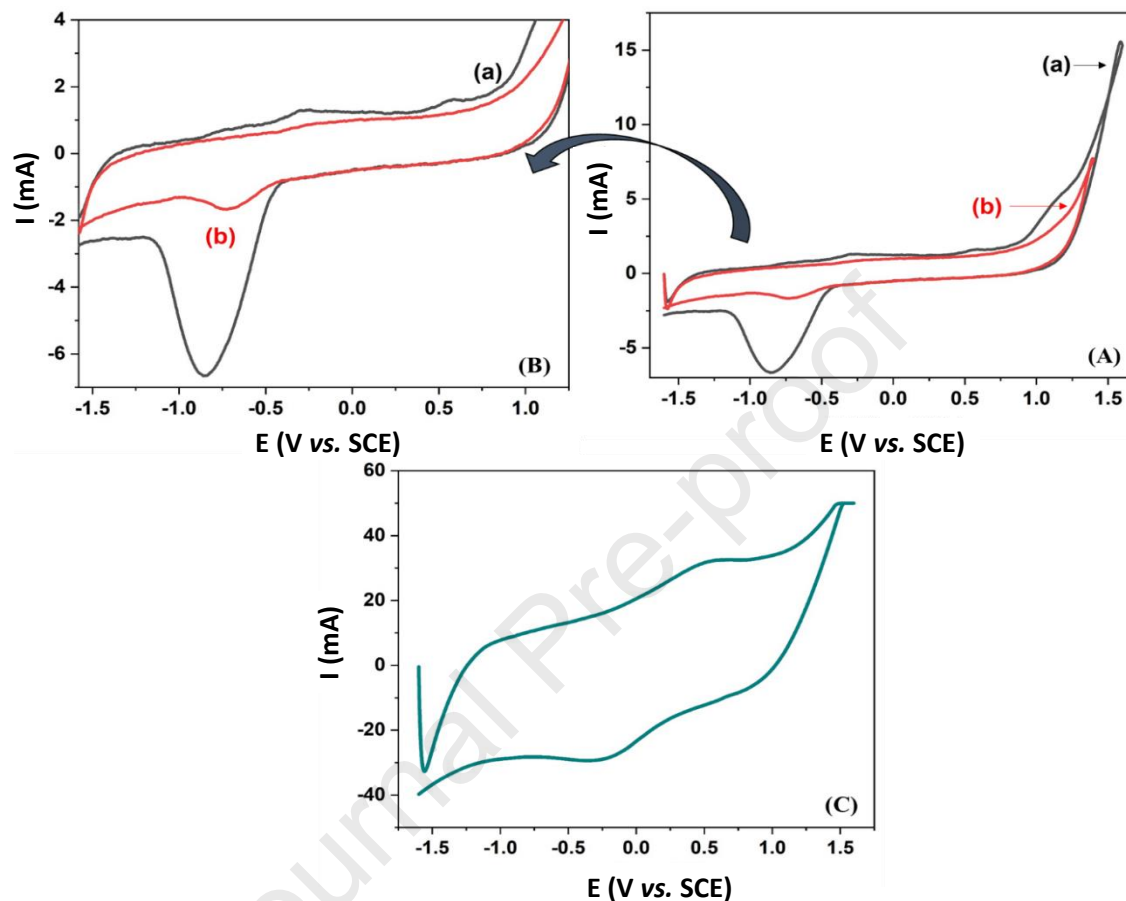
8 Electro Fenton-like oxidation was carried out in the degradation of caffeine without using
9 hydrogen peroxide at room temperature. The cyclic voltammetry (CV) recorded at a scan
10 rate of $100 \text{ mV}\cdot\text{s}^{-1}$ in the absence of Caf (black lines) and in the presence of Caf (red lines)
11 is displayed in Figure 7a and b. In the absence of Caf, two redox processes were
12 identified: one recorded at -0.30 V vs. SCE and another at 0.56 V vs. SCE . These values are
13 related to the different metal species, the first one probably attributed to the La(0)/La(III)
14 couple while the second one is attributed to Fe(II)/Fe(III) couple [24,41,51].

15 The presence of La species in the La-mordenite electrode was also studied by X and
16 al. the authors mentioned that enhances the oxidation process and a reproducible anodic
17 and cathodic peak ascribed to $\text{Fe}(\text{CN})_6^{3-}/\text{Fe}(\text{CN})_6^{4-}$ redox couple at the surface of the
18 electrode ($0.17/0.30 \text{ V vs. SCE}$) was observed, proving that La species are available for
19 the redox processes [51].

20 The oxidation of Caf (100 ppm) starts at 0.8 V vs. SCE corresponding to potential values
21 higher to that observed for Fe(III)/Fe(II) redox couple, suggesting that the presence of
22 both metal species, specially Fe(III) species, on the electrode surface improves the
23 oxidation of the compound. The cyclic voltammetry (CV) at the end of the electrolysis
24 (during 90 min) of Caf over LaFeZSM5 modified electrode in Na_2SO_4 (0.1 M) recorded

1 with a scan rate is $100 \text{ mV}\cdot\text{s}^{-1}$, suggests that the modified electrode keeps its redox
 2 process, showing the stability of the electrode (Figure 7c).

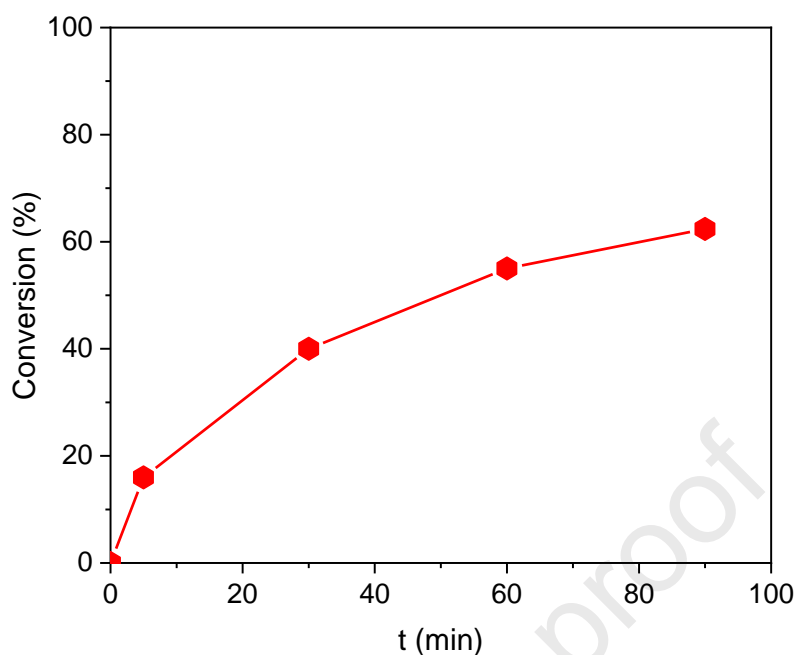
3



4

5 **Figure 7.** Cyclic voltammograms (A, B) of LaFeZSM5 modified electrode recorded at
 6 100 mV/s in the absence of Caf (a) and in the presence of Caf (100 ppm, b); (C) at the
 7 end of the electrolysis of Caf (100 ppm) at the LaFeZSM5 modified electrode in Na_2SO_4
 8 (0.1 M).

9 The electrolysis of Caf (100 ppm) on the LaFeZSM5 modified electrode at 2.0 V vs. SCE
 10 at room temperature, shows that the degradation of the pristine compound after 90 min
 11 achieves 62.4 % of conversion with 20.8 % of mineralization (Figure 8). Our results show
 12 that the electro Fenton-like oxidation increases the degradation of Caf compared with the
 13 Fenton-like reaction (51 %, 30 ppm).



1

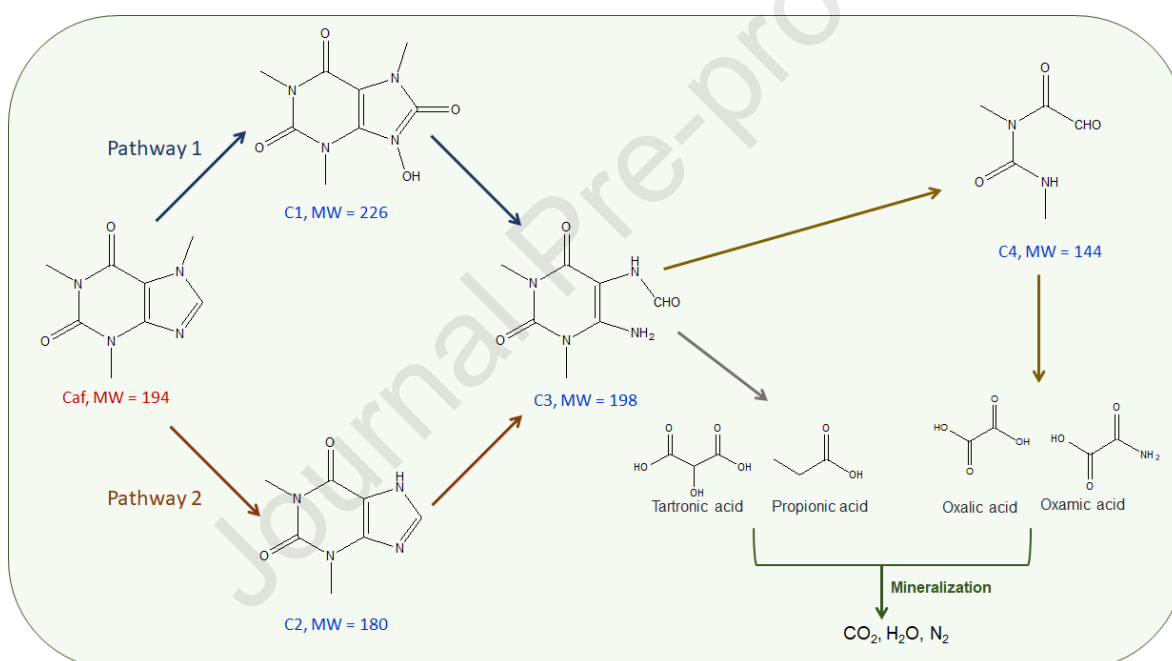
2 **Figure 8.** The evolution of the conversion of Caf in the LaFeZSM5 modified electrode.

3

4 Identification of the products during the electrolysis was carried out by HPLC-ESI/MS
5 analysis, since the initial concentration of Caf was 100 ppm, for better resolution. Such
6 analysis allowed several compounds deriving from the degradation product of Caf and to
7 suggest the formation of the intermediate products up to mineralization. The formation of
8 the intermediate compounds during Caf degradation confirms that the oxidation was
9 promoted by the electro-generation of the oxygenated radical species [42]. In both
10 Fenton-like processes, the oxidant agents are the OH^\bullet radicals, which are responsible for
11 the formation of the compounds identified up to the mineralization. 8 intermediates were
12 identified in the products of the eletrolysis, in which the C1, C2, and C3 compounds are
13 aromatic, while the C4 to C7 compounds are aliphatic. The molecular weight and the
14 structural formula of the identified products are presented in Table S4, and their ESI/MS
15 spectra are displayed in Figure S4.

1 Some of these compounds were described in the literature concerning the degradation
 2 pathways pathways of caffeine over Co-MCM41 [52]. The identified compounds and the
 3 different pathways are due to the presence of OH^\bullet and $\text{SO}_4^{\bullet-}$ radicals, which are
 4 responsible for the attack to the $\text{N}=\text{C}$ double bond of the purine structure of the Caf
 5 molecule [14,52].

6 A catalytic degradation pathway of Caf at LaFeZSM5 modified electrode could be
 7 proposed taking into account the compounds C1, C2, C3, C4, the low molecular weight
 8 organic acids, and the mineralization (Figure 9).



9

10 **Figure 9.** Proposed pathways for Fenton-like degradation of Caf molecule by LaFeZSM5.

11

12 Two pathways are proposed. Pathway 1 is comparable to one of the pathways described
 13 in [52]. The compound C1 is similar to the hydroxylated form of the 1,3,7-trimethyluric
 14 acid, which contains two additional oxygen atoms over the Caf molecule [52]. In pathway
 15 2, a new compound is proposed, C2, coming from the loss of a methyl group in the Caf
 16 molecule. Both pathways lead to C3, known as a biological metabolite of Caf [52], which
 17 is produced from C1 and C2. C3 is obtained from pathway 1 by the loss of OH and

1 protonation of N atoms, CO and methyl group. The same product is obtained from the
2 pathway 2 by the attack of the OH• radicals to the C=C bond. The generation of carbonyl
3 groups leads to the opening of the six-member ring C3 [52] with the formation of C4 that,
4 following the total opening of the ring, evolves towards the low molecular weight organic
5 acids (Table S4). These acids, identified as tartronic acid, oxamic acid, oxalic acid and
6 propionic acid by HPLC analysis, continue to suffer attacks from the radicals up to the
7 mineralization.

8

9 **4. Conclusions**

10 Three heterogeneous catalysts based in lanthanum(III) and iron(III) ions ion-exchanged
11 on two zeolite structures and a natural clay from Morocco were evaluated in Fenton-like
12 processes in order to degrade two pollutants in water, tartrazine (Tar) and caffeine (Caf).
13 The effect of different experimental parameters on both pollutants degradation was
14 determined by Box-Behenken design and high catalytic efficiency was obtained with 96.6
15 % and 51.0 % degradation of Tar and Caf, respectively, in the presence of LaFeZSM5.
16 For the best catalyst, higher mineralization rates were obtained in Fenton-like oxidation
17 with 45.5 % for Tar and 47.0 % for Caf. The degradation of Caf was improved by electro
18 Fenton-like oxidation with 62.4 % of Caf conversion after 90 min over the modified
19 LaFeZSM5 electrode. The higher conversion obtained in this work by Fenton-like
20 processes for the degradation of pollutants in water highlighted the importance of the
21 validation of the optimized experimental conditions by mathematical models.

22

23 **Conflicts of interest**

24 There are no conflicts of interest to declare.

25

1 Acknowledgements

2 O.A. thanks to ERASMUS+ Program for the mobility Ph.D. grant and O.B. thanks to
3 Fundação para Ciência e Tecnologia, Portugal (FCT) for his Ph.D. grant
4 (SFRH/BD/140362/2018). This research work has been funded by national funds funded
5 through FCT/MCTES (PIDDAC) over the projects: LA/P/0045/2020 (ALiCE),
6 UIDB/50020/2020 and UIDP/50020/2020 (LSRE-LCM), UIDB/04469/2020 (CEB) and
7 by LA/P/0029/2020 (LABELS), Centre of Chemistry (UID/QUI/0686/2020) and
8 project BioTecNorte (operation NORTE-01-0145-FEDER-000004), supported by the
9 Northern Portugal Regional Operational Programme (NORTE 2020), under the Portugal
10 2020 Partnership Agreement, through the European Regional Development Fund
11 (ERDF).

12

13 References

- 14 1. B. Zheng, J. Fan, Chen, B.; Qin, X.; Wang, J.; Wang, F.; Deng, R.; Liu, X. Rare-
15 Earth Doping in Nanostructured Inorganic Materials. *Chem. Rev.* 122 (2022)
16 5519–5603, doi:10.1021/acs.chemrev.1c00644.
- 17 2. Xin, Y.; Liu, H. Study on Mechanism of Photocatalytic Performance of La-Doped
18 TiO₂/Ti Photoelectrodes by Theoretical and Experimental Methods. *J. Solid State*
19 *Chem.* **2011**, 184, 3240–3246, doi:10.1016/j.jssc.2011.10.017.
- 20 3. Wang, L.; Ma, Y.; Wang, Y.; Liu, S.; Deng, Y. Efficient Synthesis of Glycerol
21 Carbonate from Glycerol and Urea with Lanthanum Oxide as a Solid Base
22 Catalyst. *Catal. Commun.* **2011**, 12, 1458–1462,
23 doi:10.1016/j.catcom.2011.05.027.
- 24 4. Wei, Y.; Zhang, S.; Yin, S.; Zhao, C.; Luo, S.; Au, C.T. Solid Superbase Derived
25 from Lanthanum-Magnesium Composite Oxide and Its Catalytic Performance in
26 the Knoevenagel Condensation under Solvent-Free Condition. *Catal. Commun.*
27 **2011**, 12, 1333–1338, doi:10.1016/j.catcom.2011.05.010.
- 28 5. Zheng, X.; Lin, H.; Zheng, J.; Duan, X.; Yuan, Y. Lanthanum Oxide-Modified
29 Cu/SiO₂ as a High-Performance Catalyst for Chemoselective Hydrogenation of

- 1 Dimethyl Oxalate to Ethylene Glycol. *ACS Catal.* **2013**, *3*, 2738–2749,
2 doi:10.1021/cs400574v.
- 3 6. Li, L.; Wang, X.; Zhang, Y. Enhanced Visible Light-Responsive Photocatalytic
4 Activity of LnFeO₃ (Ln = La, Sm) Nanoparticles by Synergistic Catalysis. *Mater.*
5 *Res. Bull.* **2014**, *50*, 18–22, doi:10.1016/j.materresbull.2013.10.027.
- 6 7. Liu, J.; Zhao, Z.; Xu, C. ming; Duan, A. jun Simultaneous Removal of NO_x and
7 Diesel Soot over Nanometer Ln-Na-Cu-O Perovskite-like Complex Oxide
8 Catalysts. *Appl. Catal. B Environ.* **2008**, *78*, 61–72,
9 doi:10.1016/j.apcatb.2007.09.001.
- 10 8. Chen, P.; Lei, B.; Dong, X.; Wang, H.; Sheng, J.; Cui, W.; Li, J.; Sun, Y.; Wang,
11 Z.; Dong, F. Rare-Earth Single-Atom La-N Charge-Transfer Bridge on Carbon
12 Nitride for Highly Efficient and Selective Photocatalytic CO₂ Reduction. *ACS*
13 *Nano* **2020**, *14*, 15841–15852, doi:10.1021/acsnano.0c07083.
- 14 9. Sousa-Aguiar, E.F.; Trigueiro, F.E.; Zotin, F.M.Z. The Role of Rare Earth
15 Elements in Zeolites and Cracking Catalysts. *Catal. Today* **2013**, *218–219*, 115–
16 122, doi:10.1016/j.cattod.2013.06.021.
- 17 10. Malleswara Rao, T. V.; Dupain, X.; Makkee, M. Fluid Catalytic Cracking:
18 Processing Opportunities for Fischer-Tropsch Waxes and Vegetable Oils to
19 Produce Transportation Fuels and Light Olefins. *Microporous Mesoporous Mater.*
20 **2012**, *164*, 148–163, doi:10.1016/j.micromeso.2012.07.016.
- 21 11. Mante, O.D.; Agblevor, F.A.; Oyama, S.T.; McClung, R. The Effect of
22 Hydrothermal Treatment of FCC Catalysts and ZSM-5 Additives in Catalytic
23 Conversion of Biomass. *Appl. Catal. A Gen.* **2012**, *445–446*, 312–320,
24 doi:10.1016/j.apcata.2012.08.039.
- 25 12. Chen, L.; Zhang, D.; Chen, Y.; Liu, F.; Zhang, J.; Fu, M.; Wu, J.; Ye, D. Porous
26 Stainless-Steel Fibers Supported CuCeFeO_x/Zeolite Catalysts for the Enhanced
27 CO Oxidation: Experimental and Kinetic Studies. *Chemosphere* **2022**, *291*,
28 132778, doi:10.1016/j.chemosphere.2021.132778.
- 29 13. Liu, H., Cheng, M., Liu, Y., Wang, J., Zhang, G., Li, L., Du, L., Wang, G., Yang,
30 S., Wang, X., Single atoms meet metal–organic frameworks: collaborative efforts
31 for efficient photocatalysis, *Energy Environ. Sci.*, *15* (2022) 3722, DOI:
32 10.1039/d2ee01037b
- 33 14. Shi, Q., Deng, S., Zheng, Y., Du, Y., Li, L., Yang, S., Zhang, G., Du, L., Wang, G.,
34 Cheng, M., Liu, Y., The application of transition metal-modified biochar in sulfate

- 1 radical based advanced oxidation processes, *Environmental Research* 212 (2022)
2 113340, doi.org/10.1016/j.envres.2022.113340
- 3 15. Fu, W., Yi, J., Cheng, M., Liu, Y., Zhang, G., Li, L., Du, L., Li, B., Wang, G., Yang,
4 X., When bimetallic oxides and their complexes meet Fenton-like process, *J.*
5 *Hazard. Mater.*, 424 (2022) 127419, doi.org/10.1016/j.jhazmat.2021.127419.
- 6 16. Liu, Y., Zhao, Y., Wang, J., Fenton/Fenton-like processes with in-situ production of
7 hydrogen peroxide/hydroxyl radical for degradation of emerging contaminants:
8 Advances and prospects, *J. Hazard. Mater.*, 404 (2021) 124191,
9 doi.org/10.1016/j.jhazmat.2020.124191
- 10 17. Wang, J.; Tang, J. Fe-based Fenton-like catalysts for water treatment: Preparation,
11 characterization and modification, *Chemosphere*, 276 (2021) 130177,
12 doi.org/10.1016/j.chemosphere.2021.130177.
- 13 18. Ribeiro, A.R.; Nunes, O.C.; Pereira, M.F.R.; Silva, A.M.T. An Overview on the
14 Advanced Oxidation Processes Applied for the Treatment of Water Pollutants
15 Defined in the Recently Launched Directive 2013/39/EU. *Environ. Int.* **2015**, 75,
16 33–51, doi:10.1016/j.envint.2014.10.027.
- 17 19. Fida, H.; Zhang, G.; Guo, S.; Naeem, A. Heterogeneous Fenton Degradation of
18 Organic Dyes in Batch and Fixed Bed Using La-Fe Montmorillonite as Catalyst.
19 *J. Colloid Interface Sci.* **2017**, 490, 859–868, doi:10.1016/j.jcis.2016.11.085.
- 20 20. Santos, B.L.C.; Parpot, P.; Soares, O.S.G.P.; Pereira, M.F.R.; Rombi, E.; Fonseca,
21 A.M.; Neves, I.C. Fenton-Type Bimetallic Catalysts for Degradation of Dyes in
22 Aqueous Solutions. *Catalysts* **2021**, 11, 32, doi:10.3390/catal11010032.
- 23 21. Assila, O.; Zouheir, M.; Tanji, K.; Haounati, R.; Zerrouq, F.; Kherbeche, A.
24 Copper Nickel Co-Impregnation of Moroccan Yellow Clay as Promising Catalysts
25 for the Catalytic Wet Peroxide Oxidation of Caffeine. *Heliyon* **2021**, 7, e06069,
26 doi:10.1016/j.heliyon.2021.e06069.
- 27 22. Trovó, A.G.; Silva, T.F.S.; Gomes, O.; Machado, A.E.H.; Neto, W.B.; Muller,
28 P.S.; Daniel, D. Degradation of Caffeine by Photo-Fenton Process: Optimization
29 of Treatment Conditions Using Experimental Design. *Chemosphere* **2013**, 90,
30 170–175, doi:10.1016/j.chemosphere.2012.06.022.
- 31 23. Elleuch, L.; Messaoud, M.; Djebali, K.; Attafi, M.; Cherni, Y.; Kasmi, M.; Elaoud,
32 A.; Trabelsi, I.; Chatti, A. A New Insight into Highly Contaminated Landfill
33 Leachate Treatment Using Kefir Grains Pre-Treatment Combined with Ag-Doped
34 TiO₂ Photocatalytic Process. *J. Hazard. Mater.* **2020**, 382, 121119,

- 1 doi:10.1016/j.jhazmat.2019.121119.
- 2 24. Ferreira, M.; Sahin, N.E.; Fonseca, A.M.; Parpot, P.; Neves, I.C. Oxidation of
3 Pollutants via an Electro-Fenton-like Process in Aqueous Media Using Iron-
4 Zeolite Modified Electrodes. *New J. Chem.* **2021**, *45*, 12750–12757,
5 doi:10.1039/d1nj01077h.
- 6 25. Barros, Ó.; Costa, L.; Costa, F.; Lago, A.; Rocha, V.; Vipotnik, Z.; Silva, B.;
7 Tavares, T. Recovery of Rare Earth Elements from Wastewater towards a Circular
8 Economy. *Molecules* **2019**, *24*, doi:10.3390/molecules24061005.
- 9 26. Assila, O.; Miyah, Y.; Nahali, L.; EL Badraoui, A.; Nenov, V.; EL Khazzan, B.;
10 Zerrouq, F.; Kherbeche, A. Copper-Impregnated on Natural Material as Promising
11 Catalysts for the Wet Hydrogen Peroxide Catalytic Oxidation of Methyl Green.
12 *Moroccan J. Chem.* **2021**, *9*, 084–101.
- 13 27. Assila, O.; Tanji, K.; Zouheir, M.; Arrahli, A.; Nahali, L.; Zerrouq, F.; Kherbeche,
14 A. Adsorption Studies on the Removal of Textile Effluent over Two Natural Eco-
15 Friendly Adsorbents. *J. Chem.* **2020**, *2020*, *13*, doi:10.1155/2020/6457825.
- 16 28. Ferreira, M.; Kuzniarska-Biernacka, I.; Fonseca, A.M.; Neves, I.C.; Soares,
17 O.S.G.P.; Pereira, M.F.R.; Figueiredo, J.L.; Parpot, P. Study of the
18 Electoreactivity of Amoxicillin on Carbon Nanotubes Supported Metal
19 Electrodes. *ChemCatChem* **2018**, *10*, 4914–4923, doi:10.1002/cctc.201801193.
- 20 29. Fonseca, A.M.; Goncalves, S.; Parpot, P.; Neves, I.C. Host–Guest Chemistry of
21 the (N,N'-diarylacetamidine)Rhodium(III) Complex in Zeolite Y. *Phys. Chem.*
22 *Chem. Phys.* **2009**, *11*, 6308–6314, doi:10.1039/b816698f.
- 23 30. Ahmad Bhawani, S.; Fong, S.S.; Mohamad Ibrahim, M.N. Spectrophotometric
24 Analysis of Caffeine. *Int. J. Anal. Chem.* **2015**, *2015*, *7*, doi:10.1155/2015/170239.
- 25 31. Ziylan-Yavas, A.; Ince, N.H.; Ozon, E.; Arslan, E.; Aviyente, V.; Savun-
26 Hekimoğlu, B.; Erdinçler, A. Oxidative Decomposition and Mineralization of
27 Caffeine by Advanced Oxidation Processes: The Effect of Hybridization.
28 *Ultrason. Sonochem.* **2021**, *76*, 105635, doi:10.1016/j.ultsonch.2021.105635.
- 29 32. Perveen, S.; Nadeem, R.; Iqbal, M.; Bibi, S.; Gill, R.; Saeed, R.; Noreen, S.;
30 Akhtar, K.; Mehmood Ansari, T.; Alfryyan, N. Graphene Oxide and Fe₃O₄
31 Composite Synthesis, Characterization and Adsorption Efficiency Evaluation for
32 NO₃⁻ and PO₄³⁻ Ions in Aqueous Medium. *J. Mol. Liq.* **2021**, *339*, 116746,
33 doi:10.1016/j.molliq.2021.116746.
- 34 33. Ali, M.E.M.; Abdelsalam, H.; Ammar, N.S.; Ibrahim, H.S. Response Surface

- 1 Methodology for Optimization of the Adsorption Capability of Ball-Milled
2 Pomegranate Peel for Different Pollutants. *J. Mol. Liq.* **2018**, *250*, 433–445,
3 doi:10.1016/j.molliq.2017.12.025.
- 4 34. Tabasum, A.; Zahid, M.; Bhatti, H.N.; Asghar, M. Fe₃O₄-GO Composite as
5 Efficient Heterogeneous Photo-Fenton's Catalyst to Degrade Pesticides. *Mater.*
6 *Res. Express* **2018**, 11–14, doi:10.1088/2053-1591/aae6ab.
- 7 35. Rache, M.L.; García, A.R.; Zea, H.R.; Silva, A.M.T.; Madeira, L.M.; Ramírez,
8 J.H. Azo-Dye Orange II Degradation by the Heterogeneous Fenton-like Process
9 Using a Zeolite Y-Fe Catalyst-Kinetics with a Model Based on the Fermi's
10 Equation. *Appl. Catal. B Environ.* **2014**, *146*, 192–200,
11 doi:10.1016/j.apcatb.2013.04.028.
- 12 36. Feng, J.; Hu, X.; Yue, P.L. Effect of Initial Solution PH on the Degradation of
13 Orange II Using Clay-Based Fe Nanocomposites as Heterogeneous Photo-Fenton
14 Catalyst. *Water Res.* **2006**, *40*, 641–646, doi:10.1016/j.watres.2005.12.021.
- 15 37. Reddy, C.R.; Bhat, Y.S.; Nagendrappa, G.; Jai Prakash, B.S. Brønsted and Lewis
16 Acidity of Modified Montmorillonite Clay Catalysts Determined by FT-IR
17 Spectroscopy. *Catal. Today* **2009**, *141*, 157–160,
18 doi:10.1016/j.cattod.2008.04.004.
- 19 38. Lee, H. V.; Juan, J.C.; Taufiq-Yap, Y.H. Preparation and Application of Binary
20 Acid-Base CaO-La₂O₃ Catalyst for Biodiesel Production. *Renew. Energy* **2015**,
21 *74*, 124–132, doi:10.1016/j.renene.2014.07.017.
- 22 39. Peixoto, P.; Guedes, J.F.; Rombi, E.; Fonseca, A.M.; Aguiar, C.A.; Neves, I.C.
23 Metal Ion-Zeolite Materials against Resistant Bacteria, MRSA. *Ind. Eng. Chem.*
24 *Res.* **2021**, *60*, 12883–12892, doi:10.1021/acs.iecr.1c01736.
- 25 40. Freitas, C.M.A.S.; Soares, O.S.G.P.; Órfão, J.J.M.; Fonseca, A.M.; Pereira,
26 M.F.R.; Neves, I.C. Highly Efficient Reduction of Bromate to Bromide over Mono
27 and Bimetallic ZSM5 Catalysts. *Green Chem.* **2015**, *17*, 4247–4254,
28 doi:10.1039/c5gc00777a.
- 29 41. Bencheqroun, Z.; Sahin, N.E.; Soares, O.S.G.P.; Pereira, M.F.R.; Zaitan, H.;
30 Nawdali, M.; Rombi, E.; Fonseca, A.M.; Parpot, P.; Neves, I.C. Fe (III) -
31 Exchanged Zeolites as Efficient Electrocatalysts for Fenton-like Oxidation of Dyes
32 in Aqueous Phase. *J. Envir. Chem. Eng.* **2022**, *10*, 107891,
33 doi:10.1016/j.jece.2022.107891.
- 34 42. Villalba, J.C.; Constantino, V.R.L.; Anaissi, F.J. Iron Oxyhydroxide

- 1 Nanostructured in Montmorillonite Clays: Preparation and Characterization. *J.*
2 *Colloid Interface Sci.* **2010**, *349*, 49–55, doi:10.1016/j.jcis.2010.04.057.
- 3 43. Xu, X.; Ding, Y.; Qian, Z.; Wang, F.; Wen, B.; Zhou, H.; Zhang, S.; Yang, M.
4 Degradation of Poly(Ethylene Terephthalate)/Clay Nanocomposites during Melt
5 Extrusion: Effect of Clay Catalysis and Chain Extension. *Polym. Degrad. Stab.*
6 **2009**, *94*, 113–123, doi:10.1016/j.polymdegradstab.2008.09.009.
- 7 44. Costa, F.; Silva, C.J.R.; Raposo, M.M.M.; Fonseca, A.M.; Neves, I.C.; Carvalho,
8 A.P.; Pires, J. Synthesis and Immobilization of Molybdenum Complexes in a
9 Pillared Layered Clay. *Microporous Mesoporous Mater.* **2004**, *72*, 111–118,
10 doi:10.1016/j.micromeso.2004.04.003.
- 11 45. Soares, O.S.G.P.; Marques, L.; Freitas, C.M.A.S.; Fonseca, A.M.; Parpot, P.;
12 Órfão, J.J.M.; Pereira, M.F.R.; Neves, I.C. Mono and Bimetallic NaY Catalysts
13 with High Performance in Nitrate Reduction in Water. *Chem. Eng. J.* **2015**, *281*,
14 411–417, doi:10.1016/j.cej.2015.06.093.
- 15 46. Saidian, M.; Godinez, L.J.; Prasad, M. Effect of Clay and Organic Matter on
16 Nitrogen Adsorption Specific Surface Area and Cation Exchange Capacity in
17 Shales (Mudrocks). *J. Nat. Gas Sci. Eng.* **2016**, *33*, 1095–1106,
18 doi:10.1016/j.jngse.2016.05.064.
- 19 47. Ferreira, C.; Araujo, A.; Calvino-Casilda, V.; Cutrufello, M.G.; Rombi, E.;
20 Fonseca, A.M.; Bañares, M.A.; Neves, I.C. Y Zeolite-Supported Niobium
21 Pentoxide Catalysts for the Glycerol Acetalization Reaction. *Microporous*
22 *Mesoporous Mater.* **2018**, *271*, 243–251, doi:10.1016/j.micromeso.2018.06.010.
- 23 48. Vilaça, N.; Amorim, R.; Machado, A.F.; Parpot, P.; Pereira, M.F.R.; Sardo, M.;
24 Rocha, J.; Fonseca, A.M.; Neves, I.C.; Baltazar, F. Potentiation of 5-Fluorouracil
25 Encapsulated in Zeolites as Drug Delivery Systems for in Vitro Models of
26 Colorectal Carcinoma. *Colloids Surfaces B Biointerfaces* **2013**, *112*, 237–244,
27 doi:10.1016/j.colsurfb.2013.07.042.
- 28 49. Babuponnusami, A.; Muthukumar, K. A Review on Fenton and Improvements to
29 the Fenton Process for Wastewater Treatment. *J. Environ. Chem. Eng.* **2014**, *2*,
30 557–572, doi:10.1016/j.jece.2013.10.011.
- 31 50. Sashkina, K.A.; Parkhomchuk, E. V.; Rudina, N.A.; Parmon, V.N. The Role of
32 Zeolite Fe-ZSM-5 Porous Structure for Heterogeneous Fenton Catalyst Activity
33 and Stability. *Microporous Mesoporous Mater.* **2014**, *189*, 181–188,
34 doi:10.1016/j.micromeso.2013.11.033.

- 1 51. Ismail, A.; Kawde, A.; Muraza, O.; Sanhoob, M.A.; Al-Betar, A.R. Lanthanum-
2 Impregnated Zeolite Modified Carbon Paste Electrode for Determination of
3 Cadmium (II). *Microporous Mesoporous Mater.* **2016**, *225*, 164–173,
4 doi:10.1016/j.micromeso.2015.12.023.
- 5 52. Qi, F.; Chu, W.; Xu, B. Catalytic Degradation of Caffeine in Aqueous Solutions
6 by Cobalt-MCM41 Activation of Peroxymonosulfate. *Appl. Catal. B Environ.*
7 **2013**, *134–135*, 324–332, doi:10.1016/j.apcatb.2013.01.038.
- 8

Journal Pre-proof

Highlights

- LaFe-zeolite catalysts were prepared by ion-exchanged method.
- Tartrazine and Caffeine were oxidized by Fenton-like over the heterogeneous catalysts
- Box-Behnken design was ideal to find the best degradation conditions.
- LaFeZSM5 is the utmost catalyst for Fenton-like and electro-Fenton oxidation.

Declaration of interests

The authors declare that they have no known competing financial interests or personal relationships that could have appeared to influence the work reported in this paper.

This manuscript is an original work; the results are novel and constitute an important contribution to the field of heterogeneous catalysts for the environment. The manuscript has not been published previously and is not under consideration for publication elsewhere. The work was written by the stated authors who are all aware of its content and approve its submission.

All authors declare do not have a Conflict of Interest.